

Transition Metal Complexes Coordinated by an NAD(P)H Model Compound and their Enhanced Hydride-Donating Abilities in the Presence of a Base

Atsuo Kobayashi,^[c] Hideo Konno,^[c, d] Kazuhiko Sakamoto,^[c] Akiko Sekine,^[b] Yuji Ohashi,^[b] Masashi Iida,^[a] and Osamu Ishitani*^[a]

Abstract: The ruthenium(II) and rhenium(I) complexes containing an NAD(P)H model compound, 1-benzyl-1,4-dihydronicotinamide (BNAH), as ligand, [Ru(tpy)(bpy)(BNAH)]²⁺ (**1a**) and [Re(bpy)(CO)₃(BNAH)]⁺ (**1b**), were quantitatively produced by the reaction of the corresponding metal hydrido complexes with BNA⁺ (1-benzyl-nicotinamidium cation). In the presence of base with p*K*_a = 8.9, **1a** and **1b** have much greater reducing power than “free” BNAH. The oxidation potentials of **1a** in the absence and the presence of triethylamine were 0.55 V and −0.04 V, respectively, versus Ag/AgNO₃, whereas that of “free” BNAH was 0.30 V. Spectroscopic results clear-

ly showed that the base extracts a proton from the carbamoyl group on **1a** and **1b** to give the deprotonated BNAH coordinating to the transition-metal complexes [Ru(tpy)(bpy)-(BNAH−H⁺)]⁺ (**3a**) and [Re(bpy)(CO)₃(BNAH−H⁺)] (**3b**); this deprotonation underlies the enhancement in reducing ability. The deprotonated forms **3a** and **3b** can efficiently reduce other NAD(P) models to give the corresponding 1,4-dihydro form, resulting in the deprotonated BNA⁺

being coordinated to the metal complexes [Ru(tpy)(bpy)(BNA⁺−H⁺)]²⁺ (**2a**) and [Re(bpy)(CO)₃(BNA⁺−H⁺)]⁺ (**2b**); “free” BNAH and the protonated adducts **1a** and **1b** cannot act in this way. X-ray crystallography was performed on the PF₆[−] salt of **2a**, and showed that the deprotonated nitrogen atom on the carbamoyl group coordinates to the ruthenium(II) metal center with a bond length of 2.086(3) Å. Infrared spectral data suggested that the deprotonated carbamoyl group on the reduced forms **3a** and **3b** is converted to the imido group, and that the oxygen atom coordinates to the metal center.

Keywords: acidity · coordination modes · hydrides · NADH · transition metals

[a] M. Iida, Prof. Dr. O. Ishitani
Department of Chemistry
Graduate School of Science and Engineering
Tokyo Institute of Technology, O-okayama 2-12-1
Meguro-ku 152-8551 (Japan)
Fax: (+81)3-5734-2655
E-mail: ishitani@chem.titech.ac.jp

[b] Dr. A. Sekine, Prof. Dr. Y. Ohashi
Department of Chemistry and Material Science
Graduate School of Science and Engineering
Tokyo Institute of Technology, O-okayama 2-12-1
Meguro-ku 152-8551 (Japan)

[c] Dr. A. Kobayashi, Dr. H. Konno, Prof. Dr. K. Sakamoto
Graduate School of Science and Engineering
Saitama University, 255 Shimo-Okubo
Saitama 338-8570 (Japan)

[d] Dr. H. Konno
New address
National Institute of Advanced Industrial Science and Technology
(AIST)
16-1 Onogawa, Tsukuba 305-8569 (Japan)

Supporting information for this article is available on the WWW under <http://www.chemeurj.org/> or from the author.

Introduction

It is known that the addition of metal ions promotes and accelerates many chemical reactions.^[1–2] In many cases the metal ion coordinates as a Lewis acid to a lone pair or to π electrons in a substrate, increasing the electrophilicity and oxidation capability of the substrate. Metal ions also interact with intermediates, such as radical anions, stabilizing them and, consequently, influencing reaction rates.

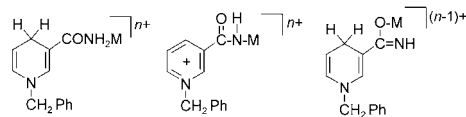
A typical example of metal-ion effects occurs in the reduction of various substrates with coenzymes NAD(P)H or their model compounds.^[3] In some enzymic systems, zinc(II) ions are essential for the reduction of unsaturated compounds with NAD(P)H.^[4] Addition of bivalent metal ions such as Mg²⁺ and Sc³⁺ dramatically accelerates the electron- or hydride-transfer rate from the NAD(P)H analogues to oxidants,^[5–20] and detailed mechanistic studies show that interaction of the oxidants and/or reduced intermediates with the metal ions is an important cause of this. It has been reported that NAD(P)H analogues also interact with metal

ions.^[5b,c,7,8a,21] The oxidation potential of a binary complex of the NAD(P)H analogue with the metal ion is shifted positively relative to the “free” NAD(P)H analogue.^[20] For example, the complex of 1-benzyl-1,4-dihyronicotinamide (BNAH, a typical NAD(P)H analogue) and Mg²⁺ is oxidized at a potential 0.23 V more positive than “free” BNAH. Consequently, the reducing abilities of the NAD(P)H analogues themselves are lessened by complexation with the metal ions, although formation of a ternary complex involving an NAD(P)H analogue, a metal ion, and an oxidant has been assumed as another cause of the acceleration.^[5,19]

We report here the unique reactivities of NAD(P)H model compounds coordinating to a ruthenium(II) or rhenium(I) complex.^[21a] They have greater reducing abilities in the presence of base than the corresponding “free” model compound. Spectroscopic studies clearly show that deprotonation from the carbamoyl group on the NAD(P)H model compound is a key stage in this “unusual” phenomenon. The X-ray crystallographic structure of the NAD(P) model compound coordinating to the ruthenium(II) complex is also reported for the first time.

Results and Discussion

As a typical run, PF₆[−] salts of 1-benzylnicotinamidium cation (BNA⁺, 32 μmol) were added to a solution of [Ru(tpy)(bpy)H]⁺PF₆[−] (32 μmol) in acetonitrile, to give a 1:1 adduct **1a** within one minute. This solution was quickly added to a further solution of triethylamine (0.2 M final concentration) and PF₆[−] salts of 1-benzyl-*N,N*-diethylnicotina-



M = [Ru(tpy)(bpy)], *n* = 2 **1a**

M = [Re(bpy)(CO)₃], *n* = 1 **1b**

2a

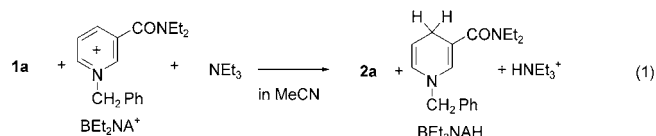
2b

3a

3b

midium cation (BEt₂NA⁺, 120 μmol) in acetonitrile under an Ar atmosphere. The solution was kept at room temperature for 1 h, and the 1,4-dihydro product of BEt₂NA⁺ (1,4-BEt₂NAH) was formed selectively; the position isomers of 1,4-BEt₂NAH and the dihydro products of BNA⁺ were not detected [Eq. (1)].

From the reaction solution, a ruthenium complex coordinated with deprotonated BNA⁺ (**2a**) was isolated at 75 %



yield. An electrospray ionization mass spectrum of **2a** showed essentially a single peak at *m/z* = 352, attributable to [Ru(tpy)(bpy)(BNA⁺−H⁺)]²⁺. In **2a**, the deprotonated N-

atom of the carbamoyl group of BNA⁺ coordinates the central ruthenium ion, according to spectroscopic evidence and X-ray crystallographic results as follows. The NMR signals of the protons at the 2- and the 4-positions of the pyridinium cation in **2a** were observed at 0.5 and 1.0 ppm downfield from those in “free” BNA⁺, respectively, but the shifts in other signals of the deprotonated BNA⁺ ligand were much smaller (<0.3 ppm). The C=O stretching band of **2a** was observed at 67 cm^{−1} lower than “free” BNA⁺, and the ν_{C−N} band for **2a** shifted up by 39 cm^{−1} (Table 1). These shifts are characteristic of deprotonated carbamoyl groups coordinating to metal complexes through the nitrogen atom.^[22]

Table 1. IR spectral data [cm^{−1}] measured in CD₃CN at room temperature.

	ν _{C5=C6}	ν _{C2=C3}	ν _{C=O}	[a]	[b]
1a	1680	1631	1530	–	1308
1a + NEt ₃ ^[c]	1679	1614	–	1563(sh)	–
1b	1680	1633	1520	–	1309
1b + NEt ₃ ^[d]	1681	1612(sh)	–	1570	–
BNAH	1687	1651	1578	–	1300
1c	1673	1590	1521	–	–
1d	1684	1646	1550	–	1284
2a	–	–	1638	–	1427
2b	–	–	1640	–	1437
BNA ⁺	–	–	1705	–	1388

[a] Medium peak, which is probably attributable to ν_{C=N}. See text. [b] Medium peak, which is probably attributable to ν_{C−N}. See text. [c] In the presence of 0.2 M NEt₃, **3a** was quantitatively formed. [d] IR bands attributed to **3b**, which was formed by deprotonation of **1b** in the presence of 0.2 M NEt₃.

This identification is clearly supported by the X-ray crystallographic analysis for the PF₆[−] salt of **2a**. Figure 1 shows the ORTEP drawing of **2a**, and selected bond lengths and angles are summarized in Table 2. The structure clearly shows that the nitrogen atom on the deprotonated carbamoyl group is directly bonded to the ruthenium center, since only a single hydrogen atom bonded to the nitrogen atom was found and the bond lengths of N6–C26 and O1–C26 were 1.315(4) and 1.234(4) Å, respectively, which are typical values for the carbamoyl group on NAD(P) model compounds (1.32 and 1.23 Å).^[23] Both the N6 and C26 atoms on the deprotonated carbamoyl group have trigonal planar structures, and the torsion angle τ[Ru–N6–C26–O1] was 4.2(5)°, showing that the lone pair of electrons on N6 and the C26–O1 double bond are highly conjugated in the same manner as the carbamoyl group on “free” 1-methylnicotinamide, in which the bond angles around the carbamoyl nitrogen atom are 124, 116, and 119°.^[23a] The pyridinium ring is almost planar and the bond lengths on it are identical to those on “free” 1-methylnicotinamide to within 0.01 Å.^[23] The torsion angle τ[C28–C27–C26–O1], which gives an indication of the conformation about the bond between the pyridinium ring and the carbamoyl group, is 18.5(4)°, similar to one of the two most stable conformations calculated theo-

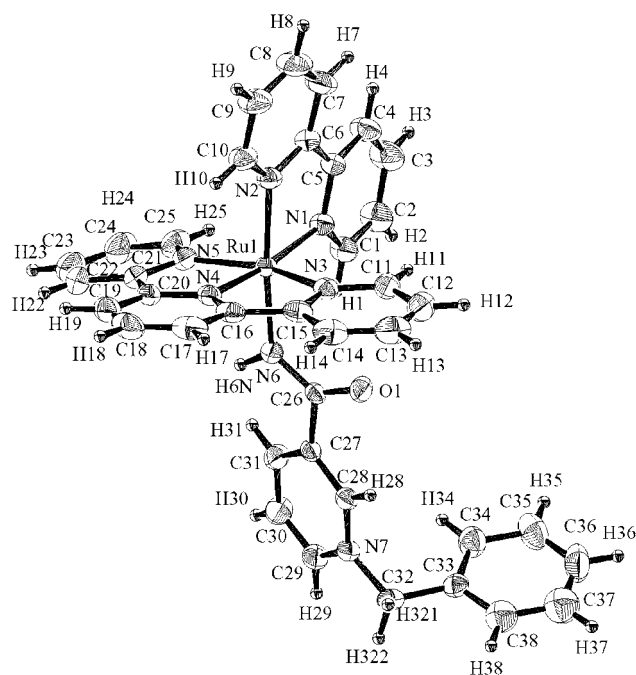


Figure 1. ORTEP view of the $[\text{Ru}(\text{tpy})(\text{bpy})(\text{BNA}^+\cdot\text{H}^+)]^{2+}$ molecule. Probability of the thermal ellipsoid is 30%. PF_6^- counterions are omitted for clarity.

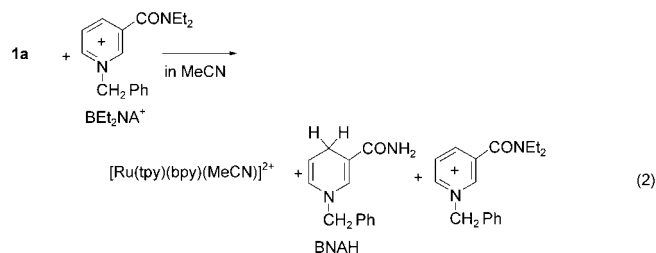
Table 2. Selected bond lengths [Å] and angles [°] for $[\text{Ru}(\text{tpy})(\text{bpy})(\text{BNA}^+\cdot\text{H}^+)](\text{PF}_6)_2$ (**2a**).

Ru1–N1	2.086(3)	Ru1–N6	2.086(3)
Ru1–N2	2.070(3)	N6–C26	1.313(4)
Ru1–N3	2.069(3)	O1–C26	1.232(4)
Ru1–N4	1.948(3)	C26–C27	1.520(4)
Ru1–N5	2.073(4)	N6–H	0.82(4)
N1–Ru1–N2	77.98(12)	C26–N6–Ru1	129.3(2)
N3–Ru1–N4	79.29(13)	O1–C26–N6	125.4(3)
N4–Ru1–N5	79.84(13)	O1–C26–C27	115.6(3)
N1–Ru1–N6	94.28(13)	N6–C26–C27	119.0(3)
N2–Ru1–N6	172.17(10)	C26–N6–H6N	115(3)
N3–Ru1–N6	93.72(13)	Ru1–N6–H6N	115(3)
N4–Ru1–N6	92.69(12)		
N5–Ru1–N6	85.08(12)		

retically (150° and 35°).^[24] The $[\text{Ru}(\text{tpy})(\text{bpy})]$ group of **2a** has a similar structure to the reported $[\text{Ru}(\text{tpy})(\text{bpy})\text{L}]^+$ type complexes ($\text{L}=\text{I}^-$, HCO_2^-),^[25] that is, slightly distorted octahedral.

The hydride transfer reaction from **1a** to BEt_2NA^+ can be followed by using ^1H NMR and IR spectroscopy, which shows that the reaction proceeds almost quantitatively, as shown in Equation (1). On the other hand, “free” 1,4-BNAH cannot reduce BEt_2NA^+ at ambient temperature, even in the presence of NEt_3 and $[\text{Ru}(\text{tpy})(\text{bpy})(\text{MeCN})]^{2+}$. In the absence of NEt_3 , quantitative splitting of **1a** proceeds in MeCN to give “free” 1,4-BNAH and $[\text{Ru}(\text{tpy})(\text{bpy})(\text{MeCN})]^{2+}$ [Eq. (2)],^[21a] but formation of **2a** and 1,4- BEt_2NAH was not observed. A similar phenomenon was observed by using a different NAD(P) model, the 1-benzyl-3-acetyl-pyridinium cation (BACPy^+) instead of BEt_2NA^+ .

These results clearly indicate that, specifically in the presence of NEt_3 , 1,4-BNAH coordinating to the ruthenium complex has greater hydride-donor ability than “free” 1,4-BNAH.



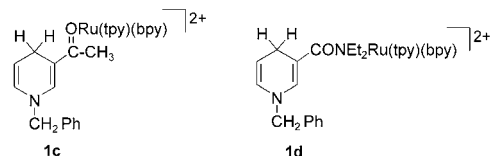
What is the crucial role of NEt_3 in the hydride-transfer reactions of **1a** to the NAD(P) models? Addition of NEt_3 to a solution of **1a** in CD_3CN caused ^1H NMR spectral changes that are summarized in Table 3 (**3a**), whereas the ^1H NMR

Table 3. ^1H NMR data of the NAD(P)H-model ligands in the complexes and “free” NAD(P)H-model.

	$\text{R}^{[b]}$	Chemical shift [ppm] ^[a]				
		2	4	5	6	$\text{CH}_2(-\text{Ph})$
1a	CONH_2	6.15	2.54	4.68	5.69	4.02
1a + NEt_3 ^[c]	CONH	6.24	2.61	4.36	5.71	4.08
1b	CONH_2	6.06	2.71	4.73	5.71	4.05
1b + NEt_3 ^[d]	CONH	6.48	2.57	4.36	5.72	4.13
BNAH	CONH_2	6.95	3.04	4.70	5.82	4.29
1c ^[e]	COCH_3	7.25	2.46	4.94	5.77	4.35
BACPyH	COCH_3	7.28	2.94	4.85	5.82	4.37
1d ^[e]	CONEt_2	5.05	2.13	3.95	5.41	3.84
BEt_2NAH	CONEt_2	5.88	2.99	4.52	5.87	4.22

[a] Numbers show the position on the dihydropyridine ring. Data were obtained from CD_3CN , and the residual protons of the solvent were used as an internal standard. [b] Substituent group on the 3-position of the dihydropyridine ring. [c] Signals attributed to **3a**, which was formed by deprotonation of **1a** in the presence of NEt_3 (0.2 M). [d] Signals attributed to **3b**, which was formed by deprotonation of **1b** in the presence of NEt_3 (0.2 M). [e] Reference [21a].

spectra of “free” 1,4-BNAH and other 1:1 adducts without a carbamoyl moiety at the 3-position, namely **1c** and **1d**,^[21] were not affected by addition of NEt_3 . In other words, the chemical shifts for the protons located close to the carbamo-



yl group of the 1,4-BNAH ligand on the 2-, 4-, and 5-positions of the dihydropyridine ring were shifted by 0.07–0.32 ppm. However the protons on the 6-position and on the benzyl group showed much smaller shifts (<0.06 ppm) upon addition of NEt_3 .

The IR bands related to the carbamoyl group and its conjugated C2–C3 double bond of **1a** also changed dramatically

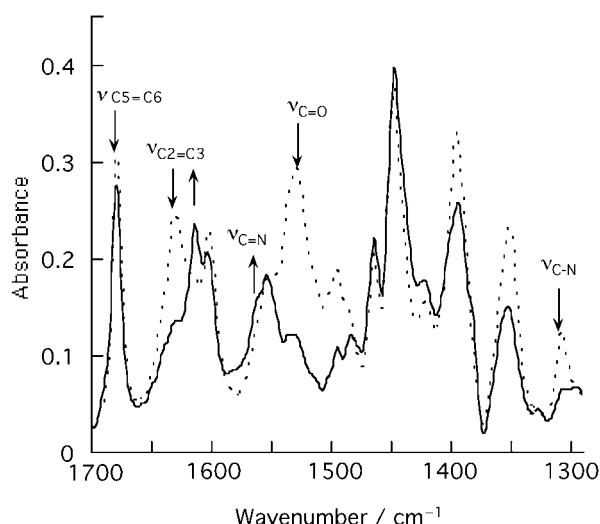
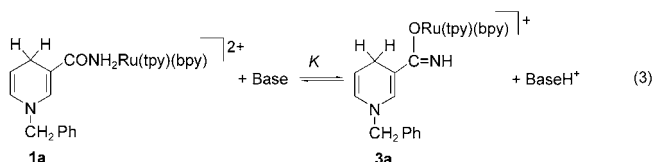


Figure 2. IR spectral change of a solution of **1a** (8.0 mM) in CD₃CN before (dotted line) and after (solid line) addition of NEt₃ (0.2 M).

with addition of NEt₃, but no shift was observed for the ν_{C5=C6} band, as shown in Figure 2. The ν_{C2=C3} band was shifted down by 17 cm⁻¹. The ν_{C=O} band, which gives as a strong peak at 1530 cm⁻¹, and a medium peak at 1308 cm⁻¹, which is probably attributable to the ν_{C-N} band in the absence of NEt₃, both disappeared, and a new medium absorption band was observed at ~1563 cm⁻¹. These results imply that NEt₃ acts as a base that takes on a proton from the carbamoyl group of **1a** to give **3a**. The coordination mode of the deprotonated 1,4-BNAH to the central ruthenium atom in **3a** should be different from **2a**, in which the deprotonated nitrogen atom of the carbamoyl group of BNA⁺ coordinates the ruthenium metal (i.e., -C(=O)-NH-Ru), as described above, since the IR bands related to the deprotonated carbamoyl groups are very different in these two complexes (Figure 2 and Table 1). The absence of the ν_{C=O} band and the medium peak at 1530 cm⁻¹ in the case of **3a** suggests that the deprotonated carbamoyl group is converted to the imide form and the oxygen atom coordinates the ruthenium, that is, -C(=NH)-O-Ru [Eq. (3)]. The new band at 1563 cm⁻¹ is probably from the C=N vibrational band.^[22]



The protonated (**1a**) and deprotonated (**3a**) forms are in equilibrium with each other in the presence of NEt₃, and also in the presence of other strong bases with (pK_a)_w = 8.9 and (pK_a)_{AN} = 17.5 (2-aminoethanol), where (pK_a)_w and (pK_a)_{AN} are pK_a values measured in aqueous solution^[26a] and in an acetonitrile,^[26b,c] respectively. For example, the ratio of **1a** and **3a** (total concentration 8.0 mM) in MeCN was 7:93 in the presence of 0.2 M NEt₃; by using these data

and Equation (4), the equilibrium constant *K* was determined as 0.5. Addition of bases with (pK_a)_w values = 7.76 and (pK_a)_{AN} = 15.9 (triethanolamine) did not change the ¹H NMR and IR spectra of **1a**. Figure 3 shows the depend-

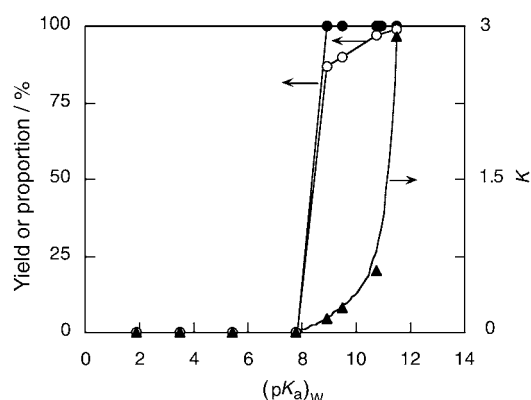


Figure 3. Dependence of (●) the yield of **2a** produced by the reaction as shown in Equation (1), (○) the proportion of **3a** in the equilibrium between **1a** and **3a** as shown in Equation (3), and (▲) the equilibrium constant between **1a** and **3a** on the (pK_a)_w value of the conjugated acid of an added base (0.2 M):^[26a] 1,10-phenantroline (1.9); nicotinic acid (3.47); pyridine (5.42); triethanolamine (7.76); 2-aminoethanol (8.9); diethanolamine (9.5); triethylamine (10.72); diethylamine (10.93); piperidine (11.5).

ence of the equilibrium constants of Equation (3) on (pK_a)_w of the bases added;^[26] from this result, the (pK_a)_{AN} value of **1a** was estimated at 18.5 ± 0.2. The coordination of 1,4-BNAH to the ruthenium complex dramatically increases the basicity of the carbamoyl group, since even the strongest base used here, piperidine, for which (pK_a)_w = 11.5 and (pK_a)_{AN} = 18.9, did not cause deprotonation from “free” 1,4-BNAH.

$$K = \frac{[\mathbf{3a}][\text{BaseH}^+]}{[\mathbf{1a}][\text{Base}]} \quad (4)$$

Figure 3 also shows the dependence of the proportion of **3a** at equilibrium with **1a** in the presence of various bases (0.2 M), and dependence of the yields of **2a**, in the reduction of BET₂NA⁺ (30 mM) with **1a** (8.0 mM) and base (0.2 M) upon the pK_a values of the added bases.^[27] Similar dependences of the equilibria and the reactivities on the added base were also observed by using BACPy⁺ instead of BET₂NA⁺ as a hydride acceptor. These results strongly imply that hydride reduction of the NAD(P) models proceeds by **3a**, but not **1a**, which dissociates to 1,4-BNAH and the solvato complex.

This claim is also supported by the observation that the adducts of [Ru(tpy)(bpy)H]⁺ with BACPy⁺ (**1c**, Tables 1 and 3), in which the substituent at the 3-position has no dissociative proton, could not reduce BET₂NA⁺ even in the presence of piperidine, and quantitatively dissociated to the corresponding 1,4-dihydro product and the solvato complex.

How much does the coordination to the ruthenium complex and deprotonation from the carbamoyl group influence the redox property of 1,4-BNAH? Figure 4 shows cyclic vol-

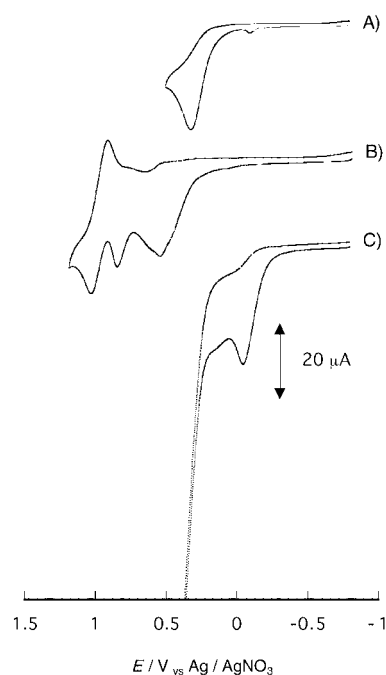


Figure 4. Cyclic voltammograms of A) 1,4-BNAH, B) **1a**, and C) **3a** (3.4 mM) in MeCN containing Et₄NBF₄ (0.1 M) under an Ar atmosphere at a scan rate of 200 mV s⁻¹. In the case of C), the solution contained 0.2 M NEt₃, and the wave at ~0.3 V is attributed to oxidation of NEt₃.

tammograms (CV) of 1,4-BNAH (A), **1a** (B), and **3a** (C) measured in MeCN or MeCN-NEt₃ (0.2 M). An irreversible anodic wave was observed at 0.32 V for oxidation of “free” 1,4-BNAH in MeCN, and addition of NEt₃ did not significantly affect the oxidation potential. On the other hand, the CV of **1a** shows two irreversible anodic waves, attributable to oxidation of the 1,4-BNAH ligand at peak potentials of 0.55 and 0.86 V, and one quasi-reversible Ru^{III}/Ru^{II} wave at 0.98 V. Unfortunately, reversible waves for the first two oxidations could not be observed even at high scan rates up to 2000 V s⁻¹. Even after an anodic scan up to 1.2 V, the following cathodic scan did not show a wave attributable to the BNA⁺ adduct **2a**, which has redox potential for Ru^{II}/Ru^{III} of 0.33 V. Although interpretation of the CV of NAD(P) model compounds is still incomplete,^[3b] it is clear that their oxidation potentials strongly reflect their reduction abilities. The NAD(P)H model compounds are known to form 1:1 complexes with metal ions, including Mg²⁺. It has been reported that the oxidation potential of 1,4-BNAH is shifted positively by ~0.2 V upon complexation with Mg²⁺.^[3b,20] It is therefore likely that the coordination of 1,4-BNAH to the central ruthenium(II) metal in **1a** causes the 0.2 V positive shift of the oxidation potential. Clearly, σ donation from the carbamoyl group of 1,4-BNAH to Ru^{II} should lower the reducing power of the 1,4-BNAH ligand in **1a**.

Addition of NEt₃ (0.2 M) caused a dramatic negative shift of the oxidation potential of the complex, as shown in Figure 4C; a first irreversible anodic wave, attributable to the oxidation of **3a**, was observed at -0.04 V versus Ag/AgNO₃, which is 0.59 V more negative than the first oxidation wave

of **1a**.^[28] Note that **3a** is oxidized at a potential 0.36 V more negative even than “free” 1,4-BNAH. This is consistent with the greater hydride-donating ability of **3a** relative to that of “free” 1,4-BNAH. We believe that this electrochemical data (Table 4) is the first clear evidence that complexation with a Lewis acid enhances the reducing power of the NAD(P)H model with the assistance of a base.

Table 4. Oxidation potentials of the complexes and “free” BNAH^[a].

	E_p^{ox} [V vs Ag/AgNO ₃] ^[b]		E_p^{ox} [V vs Ag/AgNO ₃] ^[b]
1a	0.55, 0.86, 0.98 ^[c]	3a ^[d]	-0.04
1b	0.60, 1.0	3b ^[d]	0.13
BNAH	0.32	BNAH ^[d]	0.30

[a] Cyclic voltammograms were taken in CH₃CN containing 0.1 M Et₄NBF₄ at a 0.2 V s⁻¹ scan rate, using a glassy-carbon working electrode, a Pt counter electrode, and a Ag/AgNO₃ (0.1 M) reference electrode under an Ar atmosphere. [b] Peak potentials for irreversible oxidation waves. [c] $E_{1/2}^{ox}$ for the quasi-reversible oxidation process. [d] In the presence of 0.2 M NEt₃.

The adduct of 1,4-BNAH with [Re(bpy)(CO)₃] complex **1b** is also deprotonated from the carbamoyl moiety by addition of base to give **3b**, for which the IR and ¹H NMR spectral changes are similar to those of **1a** (Tables 1 and 3). Also, IR stretching bands of the CO ligands in the deprotonated form **3b** were observed at 2011 and 1907 cm⁻¹; these values are lower by 19 and 8 cm⁻¹ than those found for **1b**. Deprotonation from the carbamoyl group coordinating to the central rhenium(I) ion should increase the charge density of the metal ion. This causes increase of π-back donation from the carbonyl ligands, and weakens the CO bonds. The difference in electrochemical properties between **1b** and **3b** is similar to the ruthenium complexes; the oxidation potential of **3b** was negatively shifted by 0.47 V relative to **1b** (Table 4).

Although these data strongly indicate that the coordinating structures of **1b** and **3b** are similar to the respective ruthenium(II) complexes **1a** and **3a**, deprotonation from **1b** is a much slower process than from **1a**. For example, 80 minutes was required after mixing **1b** and NEt₃ (0.2 M) to reach equilibrium between **1b** and **3b**, though equilibrium between **1a** and **3a** was reached within a minute, and splitting of **1b** to “free” BNAH and the solvent complex occurred competitively in this condition (Figure 5 and Scheme 1). The equilibrium constants (*K*) between **1b** and **3b** in the presence of a base were smaller than for the ruthenium complex **1a** and **3a**. For example, in the presence of 0.2 M NEt₃, *K* = 2 × 10⁻² and (p*K*_a)_{AN} = 19.9 for the rhenium complexes, and *K* = 0.6 and (p*K*_a)_{AN} = 18.5 ± 0.2 for the ruthenium complexes. The difference in charge of the central metal ions, that is, the stronger acidity of the ruthenium complex, is probably one of the causes of this difference. The local concentration of NEt₃, which has a donor number (DN)^[29] of 61 compared to 14.1 for the solvent MeCN, would be higher around the ruthenium(II) complex than around the rhenium(I) complex. In fact, using the more basic solvent

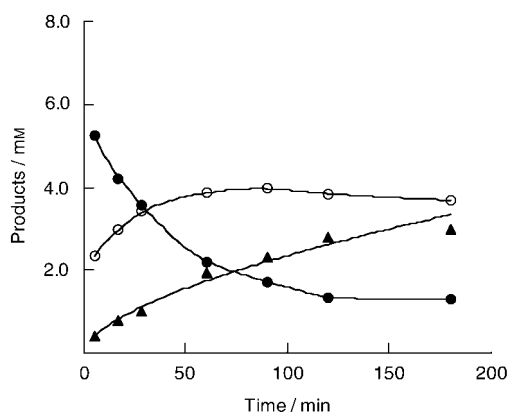
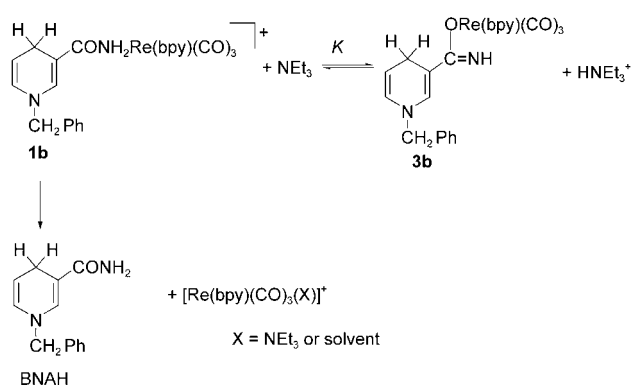


Figure 5. Reaction of **1b** (●) with NEt_3 (0.2M); yields of **3b** (○) and BNAH (▲) based on **1b** used.



Scheme 1. Reaction of **1b** in the presence of NEt_3 .

DMF ($\text{DN}=26.6$) instead of MeCN caused K between **1b** and **3b** in the presence of 0.2M NEt_3 to decrease to 2×10^{-3} .

Finally, it is noteworthy that the hydride transfer from **3a** to the NAD(P) models is also interesting as a model of “transhydrogenation” reactions between NAD and NADH by the enzyme transhydrogenase.^[30] Only the 1,4-dihydroform of the NAD(P)H models is produced by **3a** as described above,^[31] and this is the same product distribution as the enzymic reaction, whereas most other reported transhydrogenation reactions between NAD and NADH models give the 1,6- and/or 1,2-dihydro form as byproduct(s).^[32]

Conclusion

Acidity of the carbamoyl group on the BNAH increases dramatically by coordination to the ruthenium(II) or rhenium(I) complex. Addition of base ($\text{p}K_{\text{a}}^{\text{w}} > 8.9$) gives relatively stable deprotonated BNAH coordinating to the metal complex. These deprotonated BNAH– Ru^{II} and $-\text{Re}^{\text{I}}$ complexes have much stronger hydride-donating abilities and are oxidized at more negative potentials than “free” BNAH. The 1:1 adduct of the NAD(P) model and the ruthenium complex has been isolated for the first time and its structure successfully determined by X-ray crystallographic analysis.

Experimental Section

General procedures: ^1H NMR spectra were recorded on a Bruker ARX-400 NMR spectrometer (400 MHz) at 25°C. Infrared absorption spectra were recorded by JASCO FT/IR-610 spectrometers with a MCT detector at ambient temperature. Electrospray ionization mass (ESI MS) spectra were obtained by using a Mariner mass spectrometer (Applied Biosystems) with a 100 V nozzle potential. Cyclic voltammetry was carried out in an acetonitrile containing tetraethylammonium tetrafluoroborate (0.1M) as a supporting electrolyte, using an ALS/CHI CHI-620 electrochemical analyzer with a carbon working electrode (3 mm diameter), a Ag/AgNO_3 (0.01M) reference electrode, and a Pt counter electrode. A BAS C2 cell stand and a platinum (10 μm diameter) working electrode were used for rapid-scan cyclic voltammetry.

Materials: Acetonitrile was distilled over P_2O_5 three times and over CaH_2 immediately before use. Dimethylformamide (DMF) was dried over molecular sieves 4 Å and distilled at reduced pressure (~20 Torr) before use. The compound $\text{RuCl}_3 \cdot 3\text{H}_2\text{O}$ was kindly supplied by Kojima Chemical Co. The hydrido complexes: $[\text{Ru}(\text{tpy})(\text{bpy})\text{H}](\text{PF}_6) \cdot 0.5\text{H}_2\text{O}$,^[25a] and $[\text{Re}(\text{bpy})(\text{CO})_3\text{H}]$,^[33] the PF_6^- salt of the NAD(P) model compounds: BNA^+ ,^[34] BEt_2NA^+ ,^[21c,d,35] BACPy^+ ,^[21c,d] and the corresponding 1,4-dihydroforms: 1,4-BNAH,^[34] 1,4-BE $_2$ NAH,^[21c,d,35] and 1,4-BACPyH^[21c,d] were prepared according to the literature methods.

In situ preparation of 1a–d: A solution of an NAD(P) model (8.0mM) in CD_3CN (0.5 mL) was added to a solution (0.5 mL) a hydrido complex (8.0mM) in CD_3CN (0.5 mL) in an NMR tube under an argon atmosphere. After purging with argon for 1 min, the NMR tube was sealed. ^1H NMR and ESI MS data of $[\text{Ru}(\text{tpy})(\text{bpy})(\text{BNAH})]^{2+}$ (**1a**), $[\text{Re}(\text{bpy})(\text{CO})_3(\text{BNAH})]^+$ (**1b**), $[\text{Ru}(\text{tpy})(\text{bpy})(\text{BACPyH})]^{2+}$ (**1c**), and $[\text{Ru}(\text{tpy})(\text{bpy})(\text{BEt}_2\text{NAH})]^{2+}$ (**1d**) are reported in the Supporting Information of reference [21] (<http://pubs.acs.org>).

[Ru(tpy)(bpy)(BNA⁺–H⁺)](PF₆)₂ (2a**):** A hexafluorophosphate salt of BNA^+ (60 μmol) was added to a solution of $[\text{Ru}(\text{tpy})(\text{bpy})\text{H}](\text{PF}_6) \cdot 0.5\text{H}_2\text{O}$ (30 μmol) and NEt_3 (0.2M) in acetonitrile (2.0 mL). The solution was kept under dim light for 20 min at ambient temperature, then evaporated under reduced pressure at ambient temperature. The black precipitates were collected by filtration, washed twice with diethyl ether, and purified by column chromatography on aluminum oxide (Merck, eluent toluene/ CH_3CN 2:1). The main dark purple band was collected, and the solvent was removed using a rotary evaporator. The brown powder was recrystallized using $\text{CH}_3\text{CN}/\text{diethyl ether}$, then in vacuo; the typical yield was 75%. ^1H NMR (400 MHz, CD_3CN): δ = 9.57 (d, J = 5.2 Hz, 1H), 8.78 (s, 1H), 8.59 (d, J = 8.0 Hz, 1H), 8.49 (d, J = 6.0 Hz, 1H), 8.41 (d, J = 8.0 Hz, 1H), 8.34 (t, J = 8.2 Hz, 2H), 8.30 (d, J = 8.4 Hz, 2H), 8.22 (t, J = 8.0 Hz, 1H), 8.02 (t, J = 8.0 Hz, 1H), 7.84 (t, J = 8.0 Hz, 1H), 7.84 (t, J = 8.2 Hz, 5H), 7.79 (d, J = 0.4 Hz, 2H) 7.77 (d, J = 5.4 Hz, 1H), 7.68 (t, J = 5.5 Hz, 1H), 7.39 (m, 3H), 7.29 (m, 2H), 7.21 (t, J = 7.0 Hz, 2H), 7.16 (d, J = 5.0 Hz, 1H), 6.85 (t, J = 5.0 Hz, 1H), 5.56 (s, 2H), 4.69 ppm (s, 1H); elemental analysis calcd (%) for $\text{C}_{38}\text{H}_{32}\text{F}_{12}\text{N}_7\text{O}_2\text{Ru}$: C 45.93, H 3.25, O 9.87; found: C 45.86, H 3.23, O 9.50.

Crystal structure determination: A single dark-red crystal of the PF_6^- salt of **2a** was obtained by slow diffusion of diethyl ether into a solution of the complex in acetonitrile. Diffraction data was collected on a Rigaku RAPID imaging-plate diffractometer with graphite-monochromated $\text{MoK}\alpha$ radiation ($\lambda = 0.71073 \text{ \AA}$) with a crystal of size $0.25 \times 0.10 \times 0.01 \text{ mm}$ at 293 K. The intensity data were corrected for Lorentz and polarization effects. Absorption correction^[36] was applied. The structure was solved by the direct method using the TEXSAN program,^[37] and was refined on F^2 by using full-matrix least-square procedures implemented in the SHELXL-97 program.^[38] No secondary extinction corrections were applied. In the least-square refinements, all non-hydrogen atoms were refined with anisotropic displacement parameters. PF_6^- appeared to be disordered, but we did not succeed in separating the disordered structures. There are no peaks beyond 0.33 \AA^{-3} except for those around PF_6^- . The crystallographic data are as follows: $[\text{Ru}(\text{tpy})(\text{bpy})(\text{BNA}^+\text{–H}^+)](\text{PF}_6)_2$, $M_r = 962.75$, monoclinic, $P2_1/c$, $a = 14.281(18)$, $b = 26.02(3)$, $c = 11.678(10) \text{ \AA}$, $\beta = 110.48(5)^\circ$, $V = 4069(7) \text{ \AA}^3$, $Z = 4$, $\rho_{\text{calcd}} = 1.572 \text{ g cm}^{-3}$, F -

(000) = 1936, $T = 298$ K, $R = 0.044$ for 6855 reflections [$I > 2\sigma(I)$], $R = 0.061$ for all data.

CCDC-255988 contains the supplementary crystallographic data for this paper. These data can be obtained free of charge from The Cambridge Crystallographic Data Centre via www.ccdc.cam.ac.uk/data_request/cif.

Reaction of an BEt_2NA^+ with **1d in the presence of piperidine:** PF_6^- salts of BACPy^+ (32 μmol) were added to a solution of $[\text{Ru}(\text{tpy})(\text{bpy})\text{H}]^+$ (PF_6^-) (32 μmol) in acetonitrile (2 mL), to give a 1:1 adduct **1d** within 1 min. This solution was added to a solution of piperidine (0.2 M final concentration) and PF_6^- salts of BEt_2NA^+ (120 μmol) in acetonitrile under an Ar atmosphere. The solution was kept at room temperature for 1 h, and 1,4-BACPyH was formed quantitatively; however, reduction products of BEt_2NA^+ were not detected at all.

Determination of the equilibrium constants between **1 and **3**:** Both PF_6^- salts of BNA^+ (8.0 mM) and hydrido complex (8.0 mM) were dissolved in CD_3CN (0.5 mL), and the solution was quickly added to a solution of amine (0.2 M final concentration) in CD_3CN (0.5 mL). These procedures were carried out in an NMR tube under an argon atmosphere. The reaction was monitored by using ^1H NMR spectroscopy. After equilibria between **1a** and **3a**, and **1b** and **3b** were achieved, the ratio of concentration was determined from the area average of the ^1H NMR peaks at $\delta = 6.15$ and 4.68 ppm (**1a**); $\delta = 6.24$ and 4.36 ppm (**3a**); $\delta = 6.06$ and 4.73 ppm (**1b**); and $\delta = 6.48$ and 4.36 ppm (**3b**). These data and Equation (4) were used for determination of the equilibrium constants.

Acknowledgement

We acknowledge helpful discussion of Dr. Chyongjin Pac and Prof. Shunichi Fukuzumi (Osaka University). We also thank the Kojima Chemical Company for a generous gift of pure $\text{RuCl}_3 \cdot 3\text{H}_2\text{O}$. This work was partially supported by a Grant-in Aid for Scientific Research on Priority Areas (417) from the Ministry of Education, Culture, Sports, Science, and Technology (MEXT) of the Japanese Government.

- [1] For reviews see: a) S. Fukuzumi, in *Electron Transfer in Chemistry* (Ed.: V. Balzani), Wiley-VCH, Weinheim, **2001**, pp. 43–67; b) H. Yamamoto, *Lewis Acid Chemistry: A Practical Approach*, Oxford University Press, Oxford, **1999**; c) S. V. Kessar, P. Singh, *Chem. Rev.* **1997**, *97*, 721–737; d) K. Mizuno, Y. Otsuji, *Top. Curr. Chem.* **1994**, *169*, 301–346; e) *Selectivities in Lewis Acid Promoted Reactions* (Ed.: D. Schinzer), Kluwer, Boston, **1989**.
- [2] a) P. Renaud, M. Gerster, *Angew. Chem.* **1998**, *110*, 2704–2722; *Angew. Chem. Int. Ed.* **1998**, *37*, 2562–2579; b) S. Itoh, H. Kumei, S. Nagatomo, T. Kitagawa, S. Fukuzumi, *J. Am. Chem. Soc.* **2001**, *123*, 2165–2175; c) H. Ohtsu, S. Fukuzumi, *Chem. Eur. J.* **2001**, *7*, 4947–4953; d) N. Asao, T. Asano, T. Ohishi, Y. Yamamoto, *J. Am. Chem. Soc.* **2000**, *122*, 4817–4818; e) S. Fukuzumi, K. Ohkubo, *Chem. Eur. J.* **2000**, *6*, 4532–4535; f) C. L. Mero, N. A. Porter, *J. Am. Chem. Soc.* **1999**, *121*, 5155–5160; g) M. P. Sibi, J. Ji, J. B. Sausker, C. P. Jasperse, *J. Am. Chem. Soc.* **1999**, *121*, 7517–7526; h) Y. Yamamoto, S. Onuki, M. Yumoto, N. Asao, *J. Am. Chem. Soc.* **1994**, *116*, 421–422; i) S. Fukuzumi, N. Satoh, T. Okamoto, K. Yasui, T. Suenobu, Y. Seko, M. Fujitsuka, O. Ito, *J. Am. Chem. Soc.* **2001**, *123*, 7756–7766; j) S. Fukuzumi, K. Yasui, T. Suenobu, K. Ohkubo, M. Fujitsuka, O. Ito, *J. Phys. Chem. A* **2001**, *105*, 10501–10510; k) S. Fukuzumi, H. Mori, H. Imahori, T. Suenobu, Y. Araki, O. Ito, K. M. Kadish, *J. Am. Chem. Soc.* **2001**, *123*, 12458–12465; l) K. Mizuno, N. Ichinose, Y. Otsuji, *J. Org. Chem.* **1992**, *57*, 1855–1860; m) T. Tamai, K. Mizuno, I. Hashida, Y. Otsuji, *J. Org. Chem.* **1992**, *57*, 5338–5342; n) K. Mizuno, K. Terasaka, M. Ikeda, Y. Otsuji, *Tetrahedron Lett.* **1985**, *26*, 5819–8522.
- [3] For reviews see: a) C. Pac, O. Ishitani, *Photochem. Photobiol.* **1988**, *48*, 767–785; b) S. Fukuzumi, T. Tanaka, in *Photoinduced Electron Transfer Part C* (Eds.: M. A. Fox, M. Chanon), Elsevier, New York, **1988**, pp. 578–635; c) S. Yasui, M. Okamura, M. Fujii, *Rev. Heteroat. Chem.* **1999**, *20*, 145–165; d) U. Eisner, J. Kuthan, *Chem. Rev.* **1972**, *72*, 1–42; e) R. Lavilla, *J. Chem. Soc. Perkin Trans. 1* **2002**, 1141–1156.
- [4] C.-I. Branden, H. Jonvall, H. Eklund, B. Furugren, in *The Enzymes 3rd ed. Vol. 11* (Ed.: P. D. Boyer), Academic Press, New York, **1975**, pp. 103–190.
- [5] a) A. Ohno, S. Yasui, R. A. Gase, S. Oka, U. K. Pandit, *Bioorg. Chem.* **1980**, *9*, 199–211; b) A. Ohno, H. Yamamoto, T. Okamoto, S. Oka, Y. Ohnishi, *Bull. Chem. Soc. Jpn.* **1977**, *50*, 1535–1538; c) A. Ohno, S. Yasui, S. Oka, *Bull. Chem. Soc. Jpn.* **1980**, *53*, 2651–2654.
- [6] D. J. Creighton, D. S. Sigman, *J. Am. Chem. Soc.* **1971**, *93*, 6314–6316.
- [7] O. Ishitani, M. Ihama, Y. Miyauchi, C. Pac, *J. Chem. Soc. Perkin Trans. 1* **1985**, 1527–1531.
- [8] a) S. Fukuzumi, N. Nishizawa, T. Tanaka, *Chem. Lett.* **1983**, 1755–1758; b) S. Fukuzumi, Y. Fujii, T. Suenobu, *J. Am. Chem. Soc.* **2001**, *123*, 10191–10199; c) S. Fukuzumi, O. Inada, N. Satoh, T. Suenobu, H. Imahori, *J. Am. Chem. Soc.* **2002**, *124*, 9181–9188.
- [9] a) S. Shinkai, T. C. Bruice, *J. Am. Chem. Soc.* **1972**, *94*, 8258; b) S. Shinkai, T. C. Bruice, *Biochemistry* **1973**, *12*, 1750–1759.
- [10] M. Shirai, T. Chishina, M. Tanaka, *Bull. Chem. Soc. Jpn.* **1975**, *48*, 1079–1080.
- [11] R. A. Gase, G. Boxhoorn, U. K. Pandit, *Tetrahedron Lett.* **1976**, *17*, 2889–2892.
- [12] U. K. Pandit, H. van Dam, J. B. Steevens, *Tetrahedron Lett.* **1977**, *18*, 913–916.
- [13] K. Watanabe, R. Kawaguchi, H. Kato, *Chem. Lett.* **1978**, 255–258.
- [14] R. A. Gase, U. K. Pandit, *J. Am. Chem. Soc.* **1979**, *101*, 7059–7064.
- [15] A. J. De Koning, H. J. Alberts-Jansen, J. Boersma, G. J. M. Van der Kerk, *Recl. Trav. Chim. Pays-Bas* **1980**, *99*, 316–321.
- [16] J. B. Steevens, U. K. Pandit, *Tetrahedron* **1983**, *39*, 1395–1400.
- [17] J. F. J. Engbersen, A. Koudijs, H. C. V. D. Plas, *J. Org. Chem.* **1990**, *55*, 3647–3654.
- [18] N. Kanomata, T. Nakata, *Angew. Chem.* **1997**, *109*, 1263–1266; *Angew. Chem. Int. Ed. Engl.* **1997**, *36*, 1207–1211.
- [19] S. Yasui, A. Ohno, *Bioorg. Chem.* **1986**, *14*, 70–96.
- [20] S. Fukuzumi, S. Koumitsu, K. Hironaka, T. Tanaka, *J. Am. Chem. Soc.* **1987**, *109*, 305–316.
- [21] a) A. Kobayashi, R. Takatori, I. Kikuchi, H. Konno, K. Sakamoto, O. Ishitani, *Organometallics* **2001**, *20*, 3361–3363; b) H. Konno, K. Sakamoto, O. Ishitani, *Angew. Chem.* **2000**, *112*, 4227–4229; *Angew. Chem. Int. Ed.* **2000**, *39*, 4061–4063; c) H. C. Lo, O. Buriez, J. B. Kerr, R. H. Fish, *Angew. Chem.* **1999**, *111*, 1524–1527; *Angew. Chem. Int. Ed.* **1999**, *38*, 1429–1432; d) H. C. Lo, C. Leiva, O. Buriez, J. B. Kerr, M. M. Olmstead, R. H. Fish, *Inorg. Chem.* **2001**, *40*, 6705–6716; e) P. S. Wagenknecht, E. J. Sambrisk, *Recent Res. Dev. Inorg. Chem.* **2003**, *3*, 35–50; f) P. S. Wagenknecht, J. M. Penney, R. T. Hembre, *Organometallics* **2003**, *22*, 1180–1182.
- [22] a) R. J. Balahura, R. B. Jordan, *J. Am. Chem. Soc.* **1970**, *92*, 1533–1539; b) D. P. Powell, A. Woollins, *Spectrochim. Acta Part A* **1985**, *41*, 1023–1033.
- [23] a) G. R. Freeman, C. E. Bugg, *Acta Crystallogr. Sect. B* **1974**, *30*, 431–443; b) C. I. Branden, I. Lindqvist, M. Zeppezauer, *Ark. Kemi* **1968**, *30*, 41–50.
- [24] J. L. Coubeils, B. Pullman, P. Courriere, *Biochem. Biophys. Res. Commun.* **1971**, *44*, 1131–1134.
- [25] a) H. Konno, A. Kobayashi, K. Sakamoto, F. Falgale, N. E. Katz, H. Saitoh, O. Ishitani, *Inorg. Chim. Acta* **2000**, *299*, 155–163; b) M. A. Billadeau, W. T. Pennington, J. D. Petersen, *Acta Crystallogr. Sect. C* **1990**, *46*, 1105–1107.
- [26] Because the $(\text{p}K_{\text{a}})_{\text{AN}}$ values of some bases used in this study have not been reported, $(\text{p}K_{\text{a}})_{\text{w}}$ values are used in Figure 3. For $(\text{p}K_{\text{a}})_{\text{w}}$, see: a) D. R. Lide, *Handbook of Chemistry and Physics*, 73rd ed., CRC Press, Boca Raton, **1992**. For $(\text{p}K_{\text{a}})_{\text{AN}}$, see: b) K. Izutsu, *Acid-Base Dissociation Constants in Dipolar Aprotic Solvents*, Blackwell Scientific, Oxford, **1990**; c) J. F. Coetzee, G. R. Padmanabhan, *J. Am. Chem. Soc.* **1965**, *87*, 5005–5010.

- [27] "Free" 1,4-BNAH and the solvento ruthenium complex were formed in the cases of low yields of 1,4-BEt₂NAH, and total yields of 1,4-BNAH and 1,4-BEt₂NAH were almost 100% in all the cases.
- [28] The strong peak observed at > 0.21 V in Figure 4C is attributable to the oxidation of NEt₃.
- [29] V. Gutmann, E. Wychera, *Inorg. Nucl. Chem. Lett.* **1966**, 2, 257–260.
- [30] a) A. S. Pietro, N. O. Kaplan, S. P. Colowick, *J. Biol. Chem.* **1955**, 212, 941–952; b) J. B. Jackson, S. A. White, P. G. Quirk, J. D. Venning, *Biochemistry* **2002**, 41, 4173–4185; c) S. P. Colowick, N. O. Kaplan, E. F. Neufeld, M. M. Ciotti, *J. Biol. Chem.* **1952**, 195, 95–105; d) L. Ernster, C. P. Lee, *Methods Enzymol.* **1967**, 10, 729–738.
- [31] The mechanism of the regioselective transhydrogenation has not yet been clarified.
- [32] a) P. Eikeren, D. J. Grier, *J. Am. Chem. Soc.* **1977**, 99, 8057–8060; b) T. J. Von Bergen, T. Mulder, R. A. Van der Veen, R. M. Kellogg, *Tetrahedron* **1978**, 34, 2377–2383; c) T. J. Von Bergen, T. Mulder, R. M. Kellogg, *J. Am. Chem. Soc.* **1976**, 98, 1960–1962; d) Y. Ohnishi, S. Tanimoto, *Tetrahedron Lett.* **1977**, 18, 1909–1912; corrigendum: Y. Ohnishi, S. Tanimoto, *Tetrahedron Lett.* **1977**, 18, 2918; e) N. Bodor, R. Pearlman, *J. Am. Chem. Soc.* **1978**, 100, 4946–4953; f) H. Minato, T. Ito, M. Kobayashi, *Chem. Lett.* **1977**, 13–16; g) J. Ludowieg, A. Levy, *Biochemistry* **1964**, 3, 373–378.
- [33] D. H. Gibson, X. Yin, *J. Am. Chem. Soc.* **1998**, 120, 11200–11201.
- [34] D. Mauzerall, F. H. Westheimer, *J. Am. Chem. Soc.* **1955**, 77, 2261–2264.
- [35] J. P. Collman, P. S. Wagenknecht, N. S. Lewis, *J. Am. Chem. Soc.* **1992**, 114, 5665–5673.
- [36] T. Higashi, *Abscor—Empirical Absorption Correction Based on Fourier Series Approximation*, Rigaku Corporation, Tokyo, Japan, **1995**.
- [37] M. S. Corporation, TEXSAN, Program for the Crystal Structure, The Woodlands, TX 77381-5209, (USA), **2000**.
- [38] G. M. Sheldrick, SHELXS-97, Program for the Crystal Structure, University of Göttingen, Göttingen (Germany), **1997**.

Received: November 26, 2004

Revised: March 2, 2005

Published online: May 2, 2005